

REFERENCES

1. Fechner, *Schweigg, J.*, **53**, 141 (1828).
2. U. F. Franck, *Z. Elektrochem.*, **62**, 649 (1958).
3. J. J. Podestá, R. C. V. Piatti, and A. J. Arvia, *This Journal*, **126**, 1363 (1979).
4. R. S. Cooper and J. H. Bartlett, *ibid.*, **105**, 109 (1958).
5. D. Landolt, R. Acosta, R. H. Muller, and C. W. Tobias, *ibid.*, **117**, 839 (1970).
6. K. Kinoshita, D. Landolt, R. H. Muller, and C. W. Tobias, *ibid.*, **117**, 1246 (1970).
7. J. Wojtowicz, in "Modern Aspects of Electrochemistry," Vol. 8, J. O'M. Bockris and B. Conway, Editors, p. 47, Plenum Press, New York (1972).
8. P. P. Russell and J. Newman, *This Journal*, **130**, 547 (1983).
9. I. Epelboin, C. Gabrielli, M. Keddam, J.-C. Lestrade, and H. Takenouti, *ibid.*, **119**, 1632 (1972).
10. T. R. Beck, *ibid.*, **129**, 2412 (1982).

The Electrochemical Behavior of Cadmium in Sulfide Solutions

I. The Initial Stages of CdS Film Growth

Viola I. Birss* and L. Eileen Kee

Department of Chemistry, University of Calgary, Calgary, Alberta, Canada T2N 1N4

ABSTRACT

A model for the initial stages of anodic CdS film deposition in pH 14 sulfide solutions is presented. Cyclic voltammetry carried out over a range of sulfide concentrations consistently reveals three anodic peaks. The first peak has been found to represent the activation-controlled deposition of one-half of a CdS monolayer. This is substantiated by a computer-simulation of the current/potential curves based on a two-electron transfer mechanism. The Cd and S ions are then considered to place-exchange, and a second one-half monolayer of CdS is deposited in the second anodic peak. The third anodic peak depicts the completion of the place exchange of the film deposited in the second peak, and the deposition of one further complete CdS layer. This model is consistent with the measured charge densities and the dependence of anodic and cathodic current densities and potentials on the potential sweep rate. Also, the film structure developed according to this model of film initiation is consistent with the known crystal structure of bulk CdS.

There has been a great deal of interest in the last number of years in the electrochemical characteristics and behavior of CdS, primarily from the point of view of its use in heterojunction photocells (1) and in photoelectrochemical cells (2-5). Also, the photoresponses of colloidal particles of CdS, particularly when coated with deposits of Pt or RuO₂ (6), have received much attention.

In many of these cases, single crystals of CdS have been utilized (2, 4-6) and, while their photoresponses are reasonably good, there is a limitation to their use because of the cost and difficulty of preparation of single crystals on a large scale (3, 7). Also, vacuum-deposited CdS appears to be a relatively costly procedure (7). Primarily for these reasons, electrochemical methods of preparation of polycrystalline CdS films have been investigated over the last few years.

CdS films have been formed anodically (3, 8-10) by electrodeposition from alkaline sulfide solutions on various substrates. The major weaknesses of this method of CdS film preparation have been the development of a high density of recombination centers, either within the film or at the surface, and also the difficulty of forming anodic CdS films that are thick enough to be useful (8, 9). The cathodic deposition of CdS films has also been achieved (7, 11), and, by this method, thick and relatively adherent polycrystalline CdS films can be formed. However, there is a tendency towards the incorporation of minority components from solution into the CdS film, which can then result in greatly altered solid-state properties (11, 12). Also, these CdS films show a tendency towards cracking (11, 12), particularly when deposited at high current densities. Therefore, the anodic formation of CdS may still be the most practical electrochemical process and, hence, merits further study.

Previous mechanistic studies concerning the anodic formation of CdS films have been carried out by Peter (10, 13) and, subsequently, by Damjanovic (9). Both of these authors have focused their endeavors on the anodic growth of CdS at polycrystalline Cd metal from 0.1M sulfide solutions in a bicarbonate (pH = 9) medium. It was reported in their work (10) that CdS film growth commences with the deposition of one or two monolayers of film, followed by further CdS film thickening at a

rate controlled by the high field migration of Cd²⁺ ions in the CdS solid state (9, 10). This process continues until a film thickness of about 50Å is reached, at which point a change of mechanism occurs and much higher rates of reaction are observed. Therefore, these previous studies (9, 10) have validated the high field growth mechanism of anodically formed CdS films when the films range from a few monolayers to about 50Å in thickness. However, very little has been reported concerning the initial stages of film growth (up to a few monolayers) or the growth of CdS films greater than 50Å in thickness. Peter (10) reported some fine structure in the cyclic voltammograms of the "monolayer region" and has attributed this to the formation of CdS film on different crystal planes. These suppositions were tested by examining the anodic behavior of Cd/Hg amalgam electrodes (14), where some of the observed effects were ascribed to recrystallization of thin CdS films and to two-dimensional nucleation.

CdS films greater than 50Å in thickness were described (10) as growing at diffusion-limited rates, although this does not seem to be entirely consistent with the observed data.

Therefore, the object of this study has been to determine the mechanism of CdS film initiation at a polycrystalline Cd substrate, as well as to gain some understanding of the growth of CdS films thicker than approximately 50Å. The experiments reported here and in the subsequent papers of this series have been carried out with a range of sulfide concentrations in both pH 13 and pH 14 solutions, as well as in the bicarbonate medium (pH ~ 9), which has been studied previously (9, 10).

This paper focuses primarily on the initial stages of CdS film growth in pH = 14 solutions; no previous studies of CdS film growth at this pH have been reported. The subsequent papers will describe CdS film initiation in bicarbonate solutions, and also the growth of thicker CdS films in solutions of both pH 9 and pH 14.

At pH 9, the major sulfide species is considered to be HS⁻ [pK₁ = 7.0 (15, 21)], while, at pH 14, S²⁻ is likely to be the principal species [pK₂ = 11.96 (15); = 13.9 (21)].

Experimental

Cell and solutions.—The experiments were carried out in either a one- or a two-compartment cell. Solutions

* Electrochemical Society Active Member.

were made either from the $\text{Na}_2\text{S} \cdot 9\text{H}_2\text{O}$ salt or by passing H_2S through the appropriate alkaline solution. The concentration of sulfide in these solutions was determined by the titration of excess I_2 with a standardized $\text{Na}_2\text{S}_2\text{O}_3$ solution (16).

All chemicals used in this work were of reagent grade, and all water was triply distilled. The experiments reported here were carried out at room temperature, and deoxygenation of the solutions was achieved by passing nitrogen through the cell solution.

Electrodes.—A 0.8 cm diam cadmium rod of 99.999% purity (Johnson-Matthey Chemicals) was used as the working electrode. Before each experiment, the cadmium electrode was mechanically polished using 500-grade emery paper, followed by ultrasonic cleaning in acetone for 1 min and a thorough rinse with distilled water. In order to obtain a smooth and reproducible surface, the cadmium rod was then chemically polished by dipping it into a 1:1 mixture of glacial acetic acid and 30% hydrogen peroxide for 20s (10) and then ultrasonically rinsing in triply distilled water. In some cases, etching of the Cd electrode was carried out in dilute HNO_3 (13), followed by a water rinse. The cadmium rod was then coated with epoxy or wrapped in several layers of Teflon tape, leaving only the face of the rod exposed.

In order to determine the area of the Cd electrode accurately, double layer capacitance measurements (17) were made over a narrow range of potential in which no faradaic processes were expected to occur. Using a double layer capacitance for Cd of $20 \mu\text{F}/\text{cm}^2$, electrode roughness factors in the range of 1.2-2 were generally obtained. In this work, all current and charge densities are given with respect to the electrode area measured in this way.

Due to the proximity of the potential for CdS formation and reduction, and that of the hydrogen evolution reaction (HER), the cadmium rod was usually placed in the cell at an angle in order to allow hydrogen bubbles to escape freely rather than allow them to obscure varying fractions of the electrode surface during the course of the experiments.

The counterelectrode was a high area platinum gauze, and the reference electrode was either a silver/silver sulfide electrode or the RHE in a Luggin capillary. All potentials reported here are given *vs.* the RHE.

Equipment.—Standard three-electrode potentiostatic circuitry was employed, utilizing a PAR 173 potentiostat, a Tacussel G.S.A.T.P. function generator, and a Hewlett-Packard 7044A X-Y recorder. Potentiodynamic runs at high sweep rates were recorded with a Nicolet 3091 digital or a Tektronix SC 503 analog oscilloscope. Rotating disk electrode experiments were carried out with a Pine Instruments ASR Rotator.

Results and Discussion

General behavior of Cd in alkaline solutions (no sulfide).—The electrochemical behavior of cadmium in strongly alkaline solutions (no sulfide) has been extensively studied in the past (18-20), primarily due to the use of the Cd/Cd oxide electrode in Ni-Cd batteries. However, very little information regarding the potentiodynamic behavior of this electrode system has been published. Therefore, in the work reported here, cyclic voltammograms of Cd in 1M NaOH were routinely obtained prior to the addition of sulfide to the cell solution. This was done in order to ensure that the Cd oxide formation and reduction peaks would be readily recognized in the voltammograms of Cd in sulfide solutions. Also, the most accurate measurement of the Cd electrode area could be made in the alkaline solution (without sulfide) due to the wide potential range which is free of major electrochemical reactions.

A typical E/i curve for cadmium in 1M NaOH at a sweep rate (s) of 100 mV/s is shown in Fig. 1 (curve a). It can be seen that anodic current commences at a potential of about 0 mV *vs.* RHE. This is very close to the predicted potential of +5 mV for "inactive" $\text{Cd}(\text{OH})_2$ formation and +23 mV for "active" $\text{Cd}(\text{OH})_2$ (21). CdO formation is predicted to occur at a potential of about

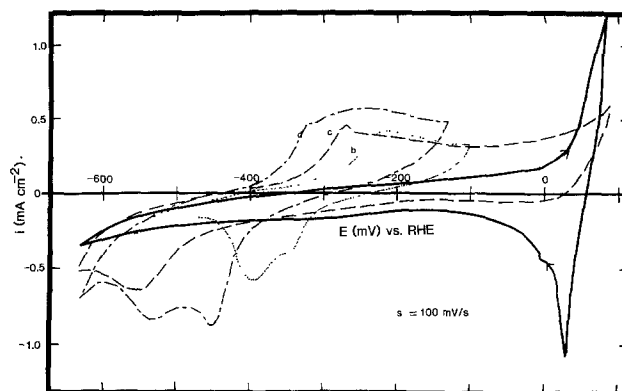


Fig. 1. Cyclic voltammograms at $s = 100 \text{ mV/s}$ for Cd rod in 1M NaOH and the following sulfide concentrations: (a) 0M (—); (b) $9 \times 10^{-4}\text{M}$ (· · ·); (c) $7 \times 10^{-3}\text{M}$ (---); and (d) $1.5 \times 10^{-1}\text{M}$ (- · - ·).

+65 mV *vs.* RHE (21) and although the anodic current observed in Fig. 1 (curve a) could be ascribed to the underpotential deposition of CdO, it seems more likely that the electrodeposition of $\text{Cd}(\text{OH})_2$ in alkaline solutions will occur first, leading to the subsequent formation of CdO with the loss of a water molecule. This is consistent with other results reported recently (22), where it was also indicated that $\text{Cd}(\text{OH})_2$ deposition precedes CdO film growth. Also, Burstein (23) found that no underpotentially deposited oxides form at a Cd anode in alkaline solutions, using the scratched electrode technique.

A measurement of the anodic and cathodic charge passed in Fig. 1 (curve a) ($Q_a/Q_c \sim 1.8$) indicates that some dissolution of Cd is likely to be occurring at potentials more positive than 0 mV *vs.* RHE. This is consistent with the supposition that $\text{Cd}(\text{OH})_2$ films form by a dissolution-precipitation (D-P) mechanism.

Curve a in Fig. 1 displays a shoulder on the rising portion of the anodic curve. Also, it is seen that film reduction occurs in two separate peaks. These observations may be related to the formation (and removal) of CdO film ($E_r \sim +65 \text{ mV vs. RHE}$). Alternatively, this may be explained by the aging of an "active" form of $\text{Cd}(\text{OH})_2$ to the "inactive" form. These two possibilities cannot readily be distinguished from our experiments.

Figure 2 shows a more complete cyclic voltammogram for Cd in this medium at $s = 200 \text{ mV/s}$. By reversing the scan at gradually more positive potentials, several other anodic shoulders and peaks appear. The anodic shoulder at $E \sim +100 \text{ mV vs. RHE}$ is probably due to CdO formation while the main peak at $\sim +250 \text{ mV vs. RHE}$ may depict a change in film growth mechanism. The current and charge densities passed in the complete sweeps in Fig. 2 are quite large, and may be responsible, in part, for the observed electrode roughening. Also, electrode roughening with successive cycles of potential would be consistent with a D-P model of film growth.

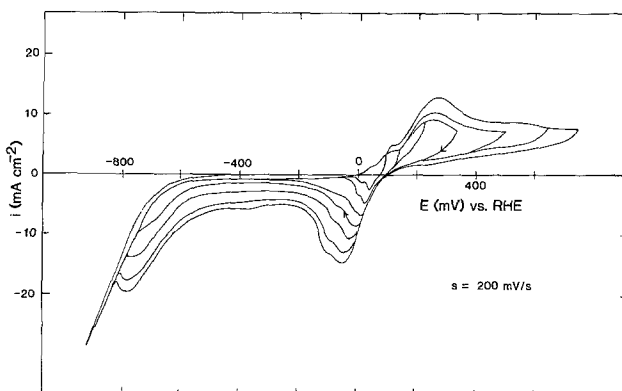
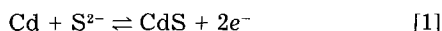


Fig. 2. E/i behavior of Cd rod in 1M NaOH; $s = 200 \text{ mV/s}$. Current increases are due to electrode roughening with cycling to more positive potentials.

General E/i behavior of Cd with addition of sulfide.—In order to observe directly the effect of added sulfide on the *E/i* response, a series of experiments was carried out in which exact aliquots of a sulfide stock solution were added to the 1M NaOH solution in the electrochemical cell. Figure 1 (curves b-d) shows a typical series of voltammograms at $s = 100$ mV/s, obtained for the various sulfide concentrations. It can be seen that a new anodic peak appears at potentials negative of Cd hydroxide formation. Upon sweep reversal, a cathodic counterpart of the anodic peak is observed. These peaks depict the formation and removal of a CdS film according to reaction [1]



In attempting to calculate the reversible potential for reaction [1] for solutions of varying sulfide concentrations, it was found that large variations exist in the literature in the reported values of E° for reaction [1]. These ranged from -1175 (24) to -1230 mV (25) vs. the NHE. Using five different sources, an average E° of -1210 mV vs. NHE was obtained.

In order to establish the experimentally observed E° for reaction [1], the potential midway between the first anodic peak (A_1) and its matching cathodic peak (C_1) was measured as a function of the concentration of S^{2-} in a 1M NaOH solution. The concentration of S^{2-} was then converted to activity in the following way. First, it is assumed that S^{2-} is the majority species (15, 21) in 1M NaOH solutions, thus preventing the need for consideration of the activity of HS^- in these calculations. However, no data is available in the literature for the mean activity coefficient, γ_{\pm} , for either S^{2-} or HS^- . Therefore, in order to convert the S^{2-} concentration to activity, the literature was reviewed for $z = -2$ ions (26), and it was found that γ_{\pm} for a number of species such as CrO_4^{2-} , CO_3^{2-} , HPO_4^{2-} , and SO_3^{2-} was in the range of 0.2-0.25. As the radius of S^{2-} is expected to be less than that of these oxyanions, γ_{\pm} for S^{2-} is likely to be at the lower end of this range. For these reasons, a value of γ_{\pm} of 0.2 was selected for the calculation and the observed potential was then plotted vs. the S^{2-} activity (Fig. 3).

It should be noted that, as the slope of Fig. 3 is approximately 30 mV per decade of S^{2-} activity, the potential varies by only 5 mV if a γ_{\pm} of 0.3 is used instead of 0.2. If γ_{\pm} were as low as 0.1, the calculated potential would be about 10 mV more positive than if γ_{\pm} were 0.2.

In extrapolating the E/S^{2-} activity plot to unity S^{2-} activity, the ionic strength of the solution would then be 2M. The literature for γ_{\pm} values for $z = -2$ ions in either a 1 or 2M solution shows only small deviations (e.g., 0.23 and 0.20 for a 1 and 2M Na_2SO_3 solution, respectively),

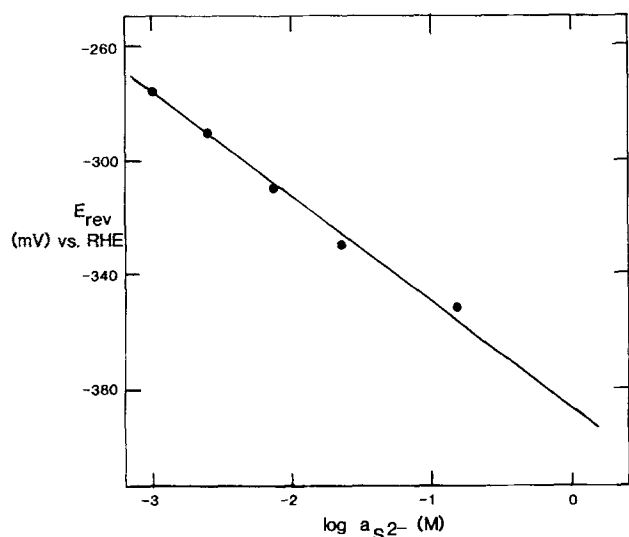


Fig. 3. Experimentally obtained (see text) reversible potentials for CdS film formation and removal vs. $\log a_{\text{S}^{2-}}$ (1M NaOH solution was utilized at all sulfide concentrations).

translating to only a 1-2 mV shift as the sulfide activity approaches 1M in a 1M NaOH solution.

E° , determined by this method from Fig. 3, was found to be -1215 mV vs. NHE (-385 mV vs. RHE at $\text{pH} = 14$). Even with an uncertainty of ± 5 mV, this value is very close to the average literature value of -1210 mV vs. NHE, and it must then be concluded that the initial deposition of CdS film is occurring approximately at the thermodynamically predicted potential. This differs from the often encountered underpotential deposition (UPD) of the first layer of a film material, e.g., Ag_2S , where an underpotential of about 120 mV is observed in the deposition of the first layer of film (27). It is also at variance with the overpotential often encountered in the case of the initial nucleation of films at an electrode surface (28).

There are several other general observations that can be made concerning curves b-d in Fig. 1. First, although the sulfide concentration has increased by a factor of about 150 from curve b to curve d, the magnitude of the currents has hardly changed. This clearly indicates that the reaction is not solution diffusion controlled, in which case the currents would have varied linearly with the sulfide concentration.

It can also be seen in Fig. 1 that, in the more dilute sulfide solutions (e.g., curve c), some Cd hydroxide film growth can still occur at ~ 0 mV vs. RHE, indicating that the CdS film is still rather thin and/or porous in nature at that potential. In contrast, in a 1.0M sulfide solution (Fig. 4), sufficient CdS film is present to 'passivate' the surface, hence preventing any Cd oxide film growth.

Effect of upper potential limit, E_+ .—Figure 5 shows a typical series of voltammograms which are obtained as E_+ is increased by small increments with each successive cycle of potential into the potential range of CdS film formation. It can be seen that three small anodic peaks appear, labeled peaks A_1 , A_2 , and A_3 , having peak potentials of E_{p,A_1} , E_{p,A_2} , and E_{p,A_3} .

It can be seen in Fig. 5 that when the anodic-going sweep is reversed at potentials that are still negative of peak A_1 , CdS reduction occurs in a single peak C_1 , having a peak potential, E_{p,C_1} , which is invariant with the amount of CdS film formed in the anodic sweep, as long as the potential had not been extended positively of A_1 . As E_{p,C_1} is constant under these conditions, the potential midway between E_{p,A_1} and E_{p,C_1} could be readily evaluated and was considered to be the empirical reversible potential of reaction [1]. Figure 6 also clearly shows that E_{p,C_1} remains constant as the film deposited in peak A_1 is reduced.

It should be noted that reversal of the potential from anodic-going to cathodic-going (Fig. 5) does not produce a continuing increase of anodic current, which is characteristic of a nucleation-controlled process (29). Instead, the current in the reverse sweep is smaller than in the

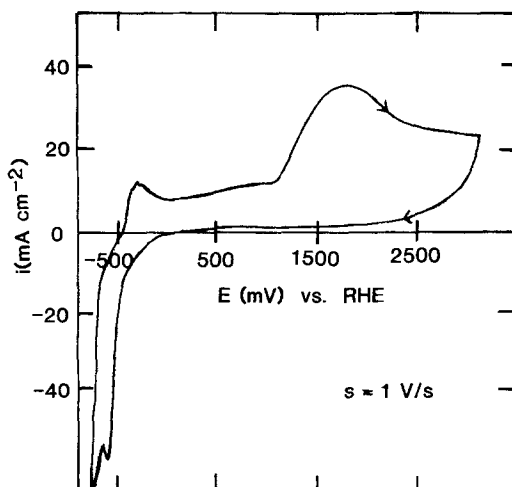


Fig. 4. In 1.0M S^{2-} , positive extension of the potential shows no evidence of Cd oxide formation; $s = 1$ V/s.

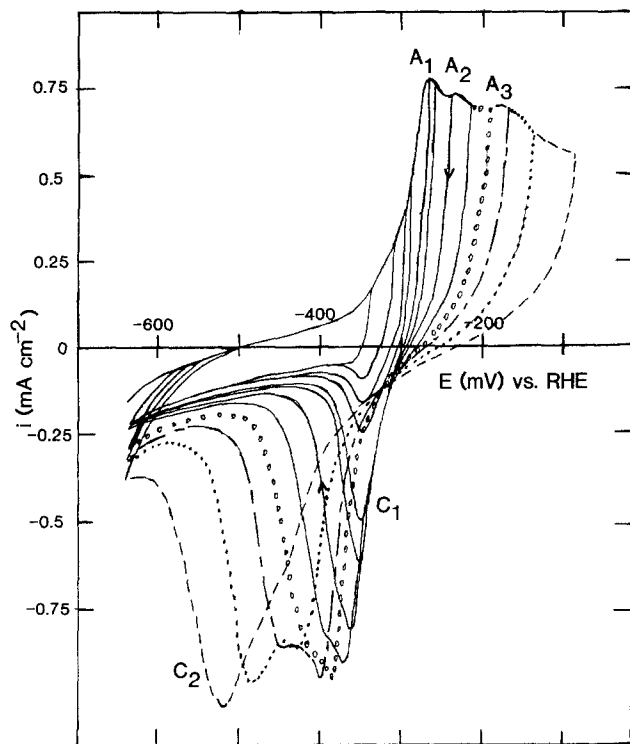


Fig. 5. Cd rod in $7 \times 10^{-3} M S^{2-} + 1M NaOH$; $s = 200$ mV/s. Peaks A_1 , A_2 , A_3 , C_1 , and C_2 can be clearly seen.

anodic-going sweep and soon becomes cathodic, as would be the case for a random deposition process at an electrode surface (29).

When E_+ is extended positively of E_{p,A_1} into peak A_2 , a second cathodic peak, C_2 , appears, initially as a shoulder on the cathodic side of C_1 , but then becoming a separate peak as more CdS film is formed. It can be seen clearly from Fig. 6 that E_{p,C_2} shifts significantly in a negative direction with an increasing amount of film produced in the anodic scan.

Further extension of the anodic potential into peak A_3 initiates a more significant hysteresis between the CdS film formation and reduction peaks (Fig. 5), so that peaks C_1 and C_2 are now both shifted negatively, with peak C_2

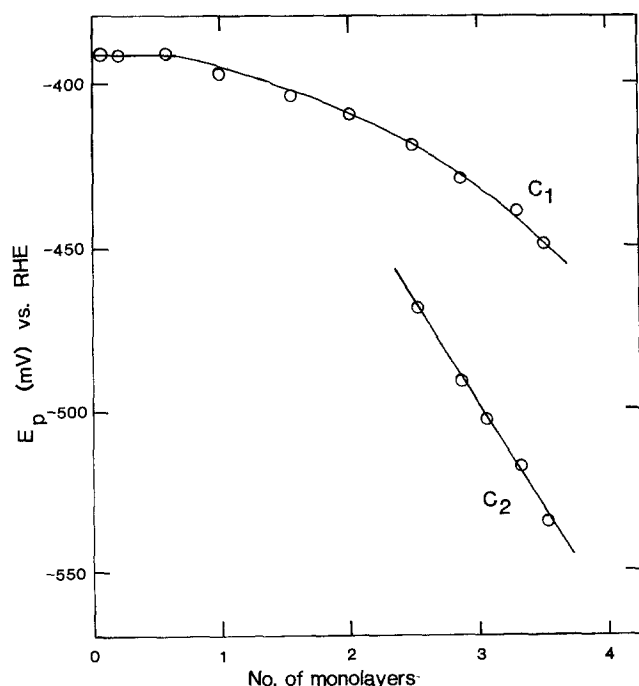


Fig. 6. Potentials of peaks C_1 and C_2 as a function of quantity of CdS film deposited. One monolayer of CdS is assumed to be $250 \mu C/cm^2$.

also increasing in magnitude as more CdS film is deposited and then removed.

It should be noted that the general appearance of peaks A_1 - A_3 , and C_1 and C_2 , as well as their dependence on the experimental variables, has been reproducible over a wide range of potential sweep rates (s from ~ 5 mV/s to ~ 10 V/s) and sulfide solution concentrations ($\sim 10^{-3}$ to $1M$).

Charge densities (peaks A_1 , A_2 , and A_3).—Because peaks A_1 - A_3 and C_1 and C_2 were observed for CdS film growth and reduction under essentially all experimental conditions, the charge density passed up to each of the anodic peaks could be readily evaluated, and some representative data are given in Table I. These charges depict the amount of anodic charge which has passed from the potential at which CdS film deposition initiates to the potential at the various peaks. No attempt was made in this work to deconvolute peaks A_1 , A_2 , and A_3 .

It can be seen that a relatively large error is associated with these charge densities, due primarily to the simultaneous occurrence of the HER in the same range of potential as the CdS peaks (Fig. 5), and hence there was difficulty in separating the charges due to these two processes. Nevertheless, from Table I, the average charge densities passed up to the potential at the three anodic peaks are given as: $q_{A_1} = 0.120 \pm 0.01$ mC/cm², $q_{A_2} = 0.230 \pm 0.03$ mC/cm², and $q_{A_3} = 0.465 \pm 0.06$ mC/cm². It should be noted that charges measured simply by integration up to the potential of peaks A_1 , A_2 , and A_3 were very similar to the cathodic charge passed when a very rapid cathodic sweep was used upon sweep reversal at E_{p,A_1} , E_{p,A_2} , and E_{p,A_3} .

These charge densities can now be compared to the expected charge density, q , for a single layer of CdS having the density of the bulk material

$$q = \left(\frac{\rho L}{M} \right)^{2/3} \frac{zF}{L} \quad [2]$$

Here, F is the Faraday constant, L is Avogadro's number, M is the molecular weight of CdS (144.5 g/mol), ρ is the density of CdS (4.82 g/cm³), and z , the number of electrons per mole, is assumed to be 2. Equation [2] yields an expected monolayer charge density of $250 \mu C/cm^2$.

With the assumption that these initial stages of CdS film growth will produce thin films of bulk CdS density, it is seen that the equivalent charge density of half a monolayer of CdS has been passed up to peak A_1 , one monolayer up to peak A_2 , and two monolayers up to peak A_3 .

Effect of potential sweep rate.—An important observation concerning the E/i behavior as exemplified in Fig. 5 is that, when the anodic sweep is reversed in the region of peak A_1 , anodic current persists until the potential has become significantly more negative than the reversible potential, and then CdS film reduction commences. This is indicative of a kinetic irreversibility in the electrodeposition and removal process in peak A_1 . The much more significant hysteresis observed between peaks A_2 and C_2 (Fig. 5) may reflect both a kinetic and a thermodynamic effect, in the sense that the nature of the film is likely to be altered or rearranged after deposition, so that a differ-

Table I. Charge densities (peaks A_1 , A_2 , and A_3)

Sulfide concentration (M)	($\mu C/cm^2$)		
	q_{A_1}	q_{A_2}	q_{A_3}
2.4×10^{-3}	0.128	0.233	0.407
7×10^{-3}	0.109	0.198	0.395
1×10^{-2}	0.113	0.226	0.566
1.5×10^{-2}	0.113	0.216	0.432
2×10^{-2}	0.128	0.235	0.423
1.5×10^{-1}	0.123	0.226	0.479
1.0	0.123	0.276	0.563
Average:	0.120	0.230	0.465

ent film structure is reduced in C_2 than is initially deposited in A_2 .

The kinetics of an electrochemical surface reaction can be studied by determining the relationship between peak potentials and the logarithm of the potential sweep rate, s . As the currents are linearly proportional to s , an $E/\log s$ study is equivalent to the evaluation of an $E/\log i$ (Tafel) relationship (30). In order to evaluate the kinetics of film deposition and removal in peaks A_1 and C_1 , *i.e.*, where the reaction is still relatively simple and no film rearrangement is likely to have occurred yet, Fig. 7 shows a plot of E_{p,C_1} vs. $\log s$, obtained from experiments in solutions of various sulfide concentrations. It was not possible to obtain an equivalent plot for peak A_1 , primarily because peak A_1 frequently appeared only as a shoulder on the cathodic side of peak A_2 .

Figure 7 shows the "Tafel" relationship for peak C_1 . At $s \geq 250$ mV/s, the slope is seen to increase relative to that at lower s , so that 250 mV/s may be considered as being close to the reversibility parameter, s_0 (31), above which the reaction is driven to complete kinetic irreversibility. Attempts to obtain accurate E_{p,C_1} data at $s < 10$ mV/s, where it would be expected that E_{p,C_1} would become independent of s (kinetically reversible), were unsuccessful due to the very pronounced interference by the HER currents, which are s -independent.

It should be noted in Fig. 7 that the E_{p,C_1} vs. $\log s$ data represented by "o" symbols were obtained by employing a constant anodic sweep rate, s_a , and varying only the cathodic sweep rate, s_c . All other data in Fig. 7 were obtained with $s_a = s_c$. The slope of the linear portion of the

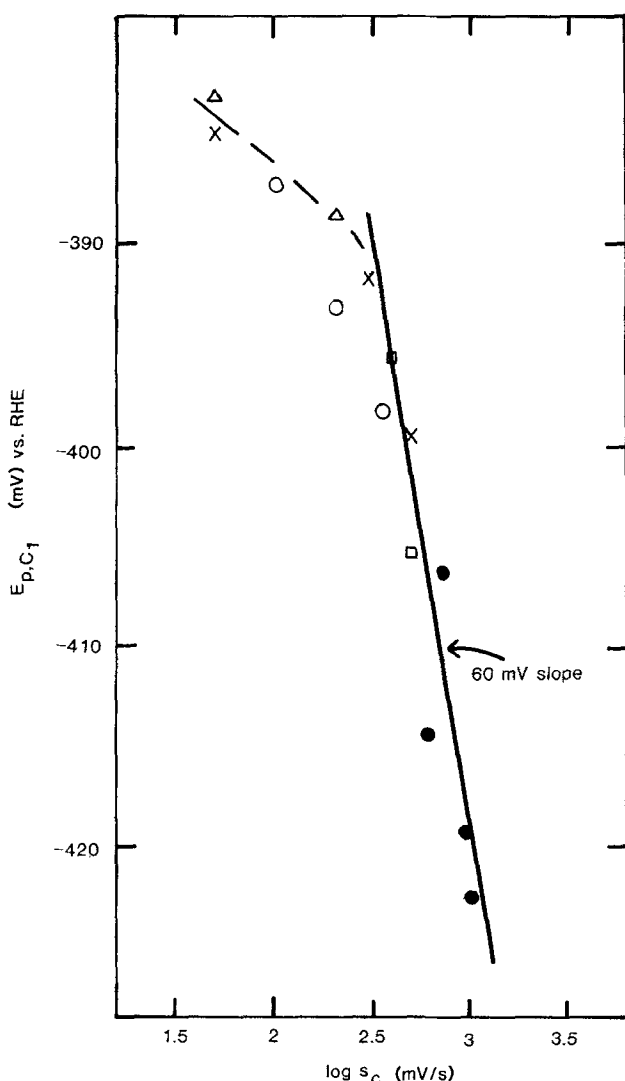


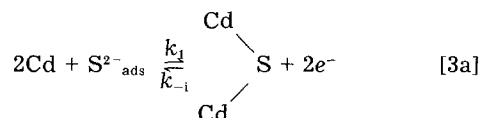
Fig. 7. Potential of peak C_1 as a function of cathodic sweep rate, s_c . Those points depicted by the "o" symbol indicate constant s_a . Other symbols depict different sets of experiments with $s_a = s_c$.

$E_{p,C_1}/\log s$ plot in Fig. 7 is very close to 60 mV/decade of s . This could be explained by a relatively simple reaction mechanism for film reduction in peak C_1 , such as the reverse of reaction [1], for which the predicted steady-state Tafel slope would be $2.3(RT/\beta zF)$, and with $z = 2$ and $\beta = 0.5$, the anticipated slope would be 59 mV. This simple mechanism would be consistent with the hypothesized absence of any film rearrangement in the peak A_1 /peak C_1 stage of CdS film deposition and removal.

A complete kinetic evaluation of peaks A_2 , A_3 , and C_2 has not yet been carried out because of the complexity of their dependence on both the charge density and on s . However, preliminary results show that the potentials of peaks A_2 and C_2 vary approximately 35 mV/decade of s , when s is in the range of 20-300 mV/s. A more detailed examination of the kinetics of CdS deposition and removal in these three peaks over a wide range of s_c , but with constant s_a , is presently being carried out. This will be the subject of a future publication.

Effect of solution agitation.—Figure 1 shows clearly that transport of sulfide ions to the Cd electrode surface is not the rate-determining process in the early stages of CdS film growth. This has been further substantiated by the results shown in Fig. 8, in which the only effect of vigorous solution agitation is the enhancement of the HER. The rate of CdS formation and reduction remains unaltered, with the CdS reduction peaks being superimposed on the now larger cathodic currents due to hydrogen production.

Model of initial stages of CdS film formation.—Peaks A_1 and C_1 .—Based primarily on the magnitude of the charge passed up to peak A_1 , 0.12 mC/cm², as well as on the invariant potential at which this film material reduces, E_{p,C_1} , it is suggested now that the first stage of CdS film formation is the deposition of half of a monolayer of sulfide ions upon the Cd surface. This will result in the formation of half of a monolayer of CdS at E_{p,A_1} .

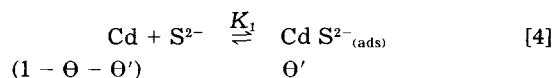


The sulfide ion is considered to be in an adsorbed state on the basis of the observed independence of the A_1 and C_1 peaks of the bulk sulfide concentration.

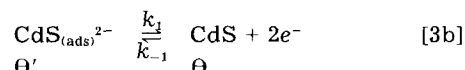
Reaction [3a] does not involve any rearrangement of the surface film. Instead, only a simple random two-dimensional deposition and removal of sulfide is considered to occur. The hysteresis observed between peaks A_1 and C_1 (Fig. 5) is therefore not due to a thermodynamic effect, but rather due to kinetic limitations. That is, the reaction is not kinetically reversible over the range of s investigated.

This will be shown below to be supported by the close match obtained between the experimentally observed peaks, A_1 and C_1 , and those obtained by a computer-simulated calculation of these curves, based on the following mechanism.

Initially, it is assumed that the sulfide ion adsorbs randomly on the Cd surface in a very fast equilibrium step



This is followed by the slow rate-determining charge transfer step (reaction [3b]), which is activation controlled



A Langmuir isotherm is used to describe those processes, with θ being the fraction of the surface that is covered by the reaction product, CdS, θ' the fraction covered by the adsorbed intermediate, $\text{CdS}^{2-}_{(\text{ads})}$, and $(1 - \theta - \theta')$ being the fraction of free Cd surface.

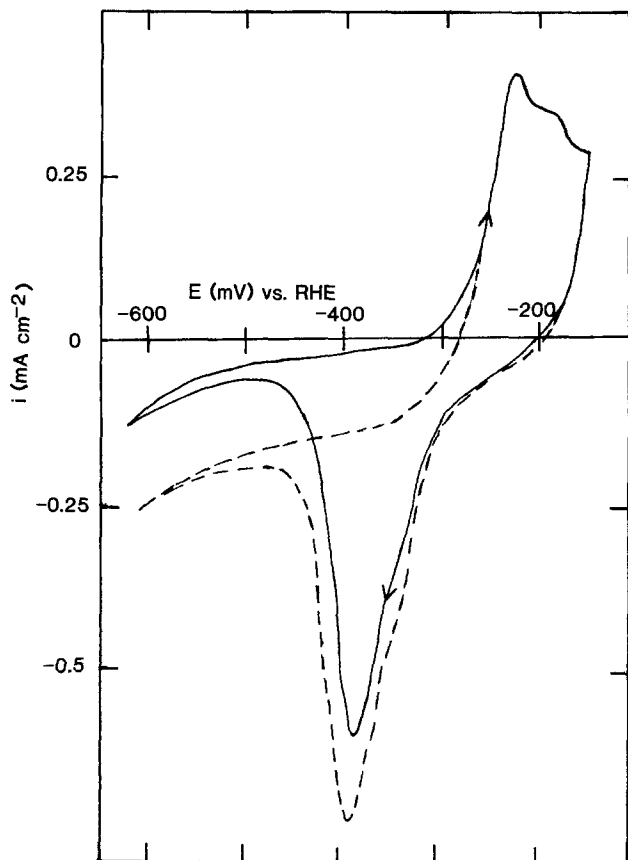


Fig. 8. Influence of solution agitation on E/i curves for CdS formation and reduction; $3 \times 10^{-3} M S^{2-}$, $s = 100$ mV/s. Quiescent (—) and stirred (---) solutions.

The faradaic current for reaction [3b] can then be expressed as in Eq. [5]

$$i = 2Fk_1 \theta' \exp\left(\frac{\beta z F E}{RT}\right) - 2F\theta k_{-1} \exp\left(\frac{-(1-\beta)z F E}{RT}\right) \quad [5]$$

where k_1 and k_{-1} are the forward and reverse rate constants for reaction [3b] at the reversible potential for reaction [1], β is the transfer coefficient and is assumed to be 1/2, z is the number of electrons, assumed to be 2, and E is the potential of the Cd electrode vs. the NHE.

It should be noted that no account has been taken in Eq. [5] of the presence of any lateral attractive or repulsive forces (32) existing between the electrodeposited surface atoms.

In order to solve Eq. [5] numerically for the current density as a function of potential, θ' must first be expressed, as in Eq. [7]

$$K_1 = \frac{\theta'}{(1 - \theta - \theta') C_{S^{2-}}} \quad [6]$$

$$\theta' = \frac{K_1 C_{S^{2-}} (1 - \theta)}{1 + K_1 C_{S^{2-}}} \quad [7]$$

where $C_{S^{2-}}$ is the bulk sulfide concentration. Equation [5] can now be rewritten, replacing θ' by the expression in Eq. [7], and this is given in Eq. [8]

$$i = \frac{2Fk_1 K_1 C_{S^{2-}} (1 - \theta)}{1 + K_1 C_{S^{2-}}} \exp\left(\frac{\beta z F E}{RT}\right) - 2F\theta k_{-1} \exp\left(\frac{-(1-\beta)z F E}{RT}\right) \quad [8]$$

$$i = A(1 - \theta) \exp\left(\frac{\beta z F E}{RT}\right) - B \theta \exp\left(\frac{-(1-\beta)z F E}{RT}\right)$$

where A and B are constant at any particular sulfide con-

centration, and are obtained numerically by trial and error in the curve simulation process.

In order to test this mechanism, a computer simulation was carried out (using Eq. [8]), of a series of voltammograms obtained experimentally by gradually increasing E_+ up to and just beyond peak A_1 , at $s = 200$ mV/s in a $0.9 M S^{2-} + 1.0 M NaOH$ solution (Fig. 9). The simulation was initiated with a θ value of 0.001 and an initial potential of -410 mV vs. RHE, the potential at which anodic current is first observed. The current density is then calculated from Eq. [8], E is then incremented by an arbitrary, but small, amount, ΔE , and θ is incremented by $\Delta\theta = i \cdot s/q \cdot \Delta E$, where q is the charge density of one CdS monolayer ($250 \mu C/cm^2$).

Figure 9 shows the calculated E/i curves in comparison with the experimental ones, and the excellent fit between them appears to support the supposition that peaks A_1 and C_1 depict the random deposition and removal of sulfide ions upon the Cd electrode surface. At the anodic peak, only half of the layer has been deposited, consistent with the observed data. After peak A_1 , a place exchange of sulfide and cadmium ions takes place, and, therefore, the experimental curves show a rising current here, while the calculated curves do not take turnover into account, and hence the currents go to zero beyond peak A_1 .

The constants, A and B (Eq. [8]), obtained by trial and error, contain the kinetic constants K_1, k_1 and k_{-1} . k_{-1} can be obtained and has a value of 3×10^{-30} mol/cm²s. K_1 and k_1 cannot be separated unless the simulation were carried out over a range of sulfide concentrations. This will be done in future work.

It should also be noted in Fig. 9 that the width of both the experimental and calculated ($z = 2$) peaks at half height, $\Delta E_{1/2}$, is about 57 mV, while the predicted $\Delta E_{1/2}$ for a model of film deposition in which $z = 1$ is about 125 mV, for irreversible conditions. This discrepancy supports our mechanism involving a two-electron transfer process (reaction [3b]) rather than a $z = 1$ mechanism, found previously for Ag_2S deposition (27) and NiS film growth (33).

Peaks A_2 and C_2 .—When the potential is extended positively of E_{p,A_1} into peak A_2 (Fig. 5), it can be seen that the cathodic reduction of CdS now occurs at increasingly negative potentials (peak C_2), in contrast to the behavior of peaks A_1 and C_1 . Also, the charge density that is passed up to E_{p,A_2} has been found to be equivalent to one monolayer of CdS film. Primarily due to the negative

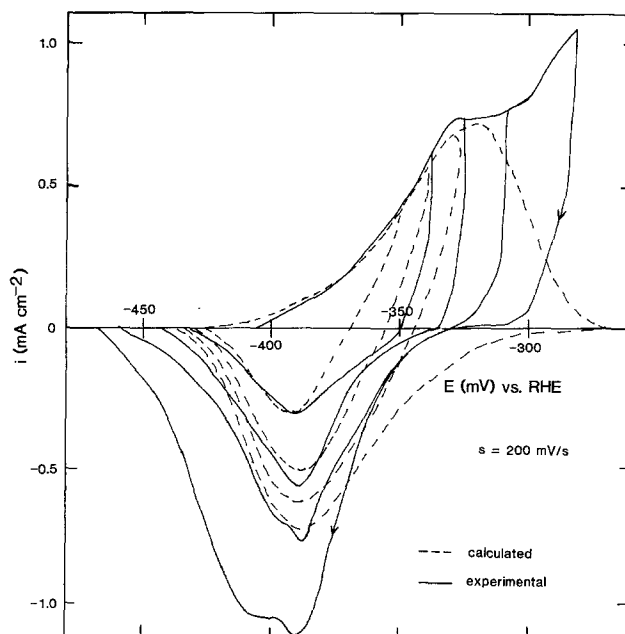


Fig. 9. Experimental (—) and calculated (---) i/E behavior at $s = 200$ mV/s at various E_1 in $0.9 M S^{2-}$. Calculated curve obtained from Eq. [8].

shift of E_{P,C_2} , it is hypothesized that, once the surface coverage exceeds one-half of a monolayer at E_{P,A_1} , a lateral repulsion between adjacent surface ions induces a place exchange process to occur. This turnover occurs by the exchange of positions of the underlying Cd ions and the surface sulfide ions. The consequence of this is that the electrode surface is now in an energetically different state upon film reduction. Now, the sulfide ions are located below the surface and an energy-requiring rearrangement is required to recover the original Cd metal surface. Therefore, the negative shift of E_{P,C_2} with increasing anodic charge density (Fig. 6) is attributed to the reduction of a more stable and transformed CdS film. When a second half of a layer of sulfide ions has deposited on the surface, and the sulfide ions deposited in peak A_1 have place-exchanged, the charge equivalent of one complete CdS monolayer has passed. This stage of film growth is marked by peak A_2 .

Peak A_3 .—The charge that passes in an anodic scan to E_{P,A_3} is formally equivalent to two monolayers of CdS. As peak A_3 is approached, the reduction peak, C_2 , continues to move more negatively with increasing anodic charge (Fig. 6). It is suggested now that peak A_3 is associated with the place exchange of the additional half-monolayer of sulfide deposited in peak A_2 and the deposition of another complete layer of sulfide ions on the electrode surface. It is reasonable that a full monolayer of sulfide would now be stable on the surface, because the significantly larger field at these more positive potentials would overcome the lateral repulsion effects thought to be present in peaks A_1 and A_2 .

Although this is only one of the numerous possible interpretations of peak A_3 , the film structure hypothesized above would be consistent with the known crystal structure of bulk CdS (34), which is expected to develop on the electrode surface as more film is deposited. CdS exists either in a wurtzite or zinc blende structure, in which alternating sheets of Cd^{2+} and S^{2-} ions exist. Each sheet of ions is displaced from its two neighboring sheets so that each ion is in a tetrahedral position.

The observed increasingly negative shift of peak C_2 is then consistent with the development of a very compact film by a place exchange mechanism. This results in a film structure that is consistent with the bulk CdS crystal structure.

Summary

This paper has focused on the initial stages of CdS film deposition and removal at a polycrystalline Cd electrode in 1.0M NaOH sulfide solutions. It has been found that, initially, the random deposition of sulfide ions is followed by the activation-controlled formation of a partial CdS monolayer. At peak A_1 , one-half of a complete CdS layer has been deposited ($\sim 125 \mu C/cm^2$). Due to lateral repulsion effects, a place exchange of Cd and S ions commences at peak A_1 , and a second one-half monolayer of CdS is deposited on the electrode surface at peak A_2 (total charge is now $\sim 250 \mu C/cm^2$). At these higher potentials, this half monolayer also place-exchanges, and now a further complete monolayer of CdS is deposited on the surface at peak A_3 , so that the equivalent of two complete monolayers of CdS film has now been formed ($\sim 500 \mu C/cm^2$).

Computer simulation methods have confirmed film initiation via a random deposition process, followed by an activation-controlled electron transfer reaction. The subsequent buildup of a compact CdS film by a field-assisted place exchange mechanism is supported by the similarity of its proposed structure with the known crystal structure of bulk CdS. It is also consistent with the field-assisted growth mechanism given in the literature (9, 10) for CdS films having thicknesses ranging from

several monolayers to about 50Å. Finally, it would also be consistent with the suggested place-exchange mechanism for Pt oxide film initiation and growth (35), as Pt oxide and CdS film growth have previously been considered to be quite similar (9).

Acknowledgments

Support of this work by the National Science and Engineering Research Council of Canada is gratefully acknowledged. Thanks are also due to the Alberta Summer Temporary Employment Program for the funding of one of us (E.K.).

Manuscript submitted May 2, 1985; revised manuscript received March 18, 1986.

REFERENCES

1. K. W. Boer, *Phys. Rev. B*, **13**, 5373 (1976).
2. R. A. L. Vanden Berghe, W. P. Gomes, and F. Cardon, *Ber. Bunsenges*, **77**, 289 (1973).
3. B. Miller and A. Heller, *Nature*, **262**, 680 (Aug. 1976).
4. A. Heller, K. C. Chang, and B. Miller, *This Journal*, **124**, 697 (1977).
5. H. Gerischer and J. Gobrecht, *Ber. Bunsenges*, **82**, 520 (1978).
6. W. Gissler, A. J. McEvoy, and M. Graetzel, *This Journal*, **129**, 1733 (1982).
7. G. P. Power, D. R. Peggs, and A. J. Parker, *Electrochim. Acta*, **26**, 681 (1981).
8. B. Miller, S. Menezes, and A. Heller, *J. Electroanal. Chem.*, **85** (1979).
9. L.-S. Yeh, P. G. Hudson, and A. Damjanovic, *J. Appl. Electrochem.*, **12**, 153 (1982).
10. L. M. Peter, *Electrochim. Acta*, **23**, 165 (1980).
11. W. R. Fawcett, *This Journal*, **128**, 963 (1981).
12. A. S. Baranski and W. R. Fawcett, *ibid.*, **127**, 766 (1980).
13. L. M. Peter, *ibid.*, **23**, 1073 (1978).
14. M. I. Da Silva Pereira and L. M. Peter, *J. Electroanal. Chem.*, **140**, 103 (1982).
15. "CRC Handbook of Chemistry and Physics," 55th ed. (1974-1975).
16. "Vogel's Textbook of Quantitative Inorganic Analysis," Longman Group, Ltd., Essex, England (1978).
17. M. Babai, T. Tshernikovskii, and E. Gileadi, *This Journal*, **119**, 1018 (1972).
18. M. W. Breiter and J. L. Weininger, *ibid.*, **113**, 651 (1966).
19. R. D. Armstrong, K. Edmonson, and G. D. West, "Electrochemistry," Vol. 4, Chap. 2, The Chemical Society, London (1974).
20. M. W. Breiter, *Electrochim. Acta*, **22**, 1219 (1977).
21. M. Pourbaix, "Atlas of Electrochemical Equilibria in Aqueous Solutions," NACE, Houston, TX (1974).
22. J. A. Garrido Ponce, *An. Quim. Ser. A*, **78**, 268 (1982).
23. G. T. Burstein, *This Journal*, **130**, 2133 (1983).
24. G. Milazzo and S. Caroli, "Tables of Standard Electrode Potentials," pp. 100-105, John Wiley and Sons, New York (1978).
25. W. M. Latimer, "The Oxidation States of the Elements and their Potentials in Aqueous Solutions," Prentice-Hall, New York (1938).
26. V. M. M. Lobo and J. L. Quaresma, "Electrolyte Solutions: Literature Data on Thermodynamic and Transport Processes," Vol. II, Coimbra, Portugal (1981).
27. V. I. Birss and G. A. Wright, *Electrochim. Acta*, **27**, 1 (1982).
28. V. I. Birss and G. A. Wright, *ibid.*, **27**, 1429 (1982).
29. H. Angerstein-Kozłowska, B. E. Conway, and J. Klinger, *J. Electroanal. Chem.*, **87**, 301 (1978).
30. E. Gileadi and S. Srinivasan, *Electrochim. Acta*, **11**, 321 (1966).
31. H. Angerstein-Kozłowska and B. E. Conway, *ibid.*, **95**, 1 (1979).
32. H. Angerstein-Kozłowska, J. Klinger, and B. E. Conway, *ibid.*, **75**, 45 (1977).
33. M. Kesten, *Corrosion*, **32**, 94 (1976).
34. R. C. Evans, "An Introduction to Crystal Chemistry," Cambridge University Press, New York (1966).
35. H. Angerstein-Kozłowska, B. E. Conway, and W. B. A. Sharp, *J. Electroanal. Chem.*, **43**, 9 (1973).